Journal of Electronic Materials (2023) 52:2303–2311
https://doi.org/10.1007/s11664-023-10265-5

ORIGINAL RESEARCH ARTICLE

# Interface Passivation of Perovskite Solar Cells by Fmoc-Ala-OH Amino Acids

**Jian Song[1] · Linlin Wang[2] · Qiaopeng Cui[1] · Aixiang Song[1] · Qiannan Yao[1] · Zhenmei Shao[2] · Chunguang Ren[3]**

Received: 2 August 2022 / Accepted: 19 January 2023 / Published online: 11 February 2023


## Abstract

Carrier recombination at the interfaces of perovskite solar cells (PSCs) has always been one of the main limitations of device performance. How to restrain the generation of defect state on the perovskite film surface and improve the carrier extraction efficiency are crucial to break the bottleneck. Herein, the influence of an amino acid-based N-(9-fluorenylmethoxycarbonyl)-L-alanine (Fmoc-Ala-OH) molecule on the perovskite surface quality and thus device performance were investigated. Varied concentrations (0 mg/mL, 0.5 mg/mL, 1 mg/mL, 1.5 mg/ mL, 2 mg/mL) of Fmoc-Ala-OH were explored, and 1.5 mg/mL was found to be the optimal passivation concentration for perovskite films. This strategy could reduce $PbI_2$ impurity, prolong carrier lifetime, and enhance luminescence of perovskite films. Space charge limited current results indicated a lower defect state density on the perovskite film surface. Electrochemical impedance spectroscopy revealed a decreased charge transfer resistance and an increased recombination resistance after amino acid passivation. As a result, a power conversion efficiency of 21.14% with a high $V_{oc}$ of 1.08 V was obtained for the modified device.

**Keywords** Amino acid · Fomc-Ala-OH · interface passivation · perovskite solar cells

## Introduction

Solar cells and solar energy application exhibit a huge influence in reducing climate change and protecting the environment.[1,2] In functional materials for solar cells, perovskite materials have aroused tremendous research interest due to their superior light absorption performance, ambipolar carrier transport and adjustable band gap.[3–6] These novel properties open a window for solar cell structural design. In just 10 years of development, the photoelectric conversion efficiency (PCE) of perovskite solar cells (PSC) has exceeded 25%, and its thermal and chemical stability have been greatly improved, presenting advantages both in photovoltaic performance and cost compared to silicon solar cells.[7] At present, the state-of-the-art PSCs utilize conventional or inverted heterojunction structure.[8,9] In inverted structure, the interfaces of electron transport layer (ETL) and hole transport layer (HTL) with perovskite film are prerequisites for constructing high-performance solar cells.[10] A suitable carrier transport layer (CTL) can effectively extract carriers and minimize the non-radiative recombination at interfaces.[11] Currently, organic[6,6]-phenyl-C61-butyric acid methyl ester (PCBM) and inorganic nickel oxide (NiO) are the most popular ETL and HTL in inverted PSCs, which also have a good match with the perovskite layer.

Because of the amazing defect tolerance of perovskite materials, the carriers usually have long diffusion length. However, there are a large number of defects on the grain boundary and surface of perovskite films.[12] The PCE of inverted planar PSCs is still relatively lower than the conventional one, and experimental studies have demonstrated that trap states and local electronic states are main factors. It has been shown that carrier recombination at the CTL/

✉ Linlin Wang
wanglinlin@sdbi.edu.cn

✉ Zhenmei Shao
shaozhenmei@sdbi.edu.cn

✉ Chunguang Ren
cgren@ytu.edu.cn

[1] The Jiangsu Province Engineering Laboratory of High Efficient Energy Storage Technology and Equipments, School of Materials Science and Physics, China University of Mining and Technology, Xuzhou 221116, China

[2] Department of Food Engineering, Shandong Business Institute, Yantai 264670, China

[3] College of Life Sciences, Yantai University, Yantai 264005, China

perovskite interfaces is a determining factor for the device performance capabilities.[13] Therefore, a simple and effective avenue to suppress these trap states is essential to improving the performance of PSCs. To date, many research efforts have been made to improve the quality of perovskite films, such as adding organic molecules, Lewis acids/bases, metal ions and other materials to the precursor solution to improve crystallinity of perovskite film and reduce the total grain boundary area, which can further substantially decrease the trap states on the surface of perovskite film.[14–17] Tang et al. introduced $CH_3NH_3PbBr_3$ quantum dots into anti-solvent to provide uniform nucleation sites, and the increased crystallinity of $CH_3NH_3PbI_3$ film extended corresponding carrier lifetime.[18] Some additives can reduce the crystallization rate to further increase the particle size. Yan et al. used $Pb(CH_3COO)_2$ as an additive to make the perovskite mesophase more stable, delaying the crystallization process and improving the morphology of the perovskite film.[19] Gong's group proposed to use aminopropanoic acid (APPA) as an additive to directly adjust the crystal growth process and reduce the defects of the perovskite film.[20] Liu et al. employed an organic amine compound to passivate the ionic defects on the surface of perovskite films, raising the solar cell efficiency from 18.56% to 20.06%.[21] Chen et al. reported potassium bis(fluorosulfonyl) imide as an effective passivator for perovskite films, in which not only S = O and S–N bonds but also charged $K^+$ and $FSI^-$ ions contribute to the passivation of multiple defects in perovskite films.[22] Zhang et al. proposed a systematic passivation strategy, using L-aspartic acid buffer layer, cross-linking sodium glycinate additive and 2-hydroxyacetophenone to modify the bottom, inner and top parts of perovskite films.[23] Although numerous approaches have been applied, the passivation of trap states at grain boundaries still remains a great challenge because of the diversity of surface defects. In fact, most passivation molecules have only one or two functional groups, which are not sufficient to passivate the complex defects.

Amino acids are a class of small molecules composed of C, H, and O, with a variety of side chain groups. These different functional groups can passivate various defects on the surface of the perovskite film.[24,25] Specifically, amines ($-NH_2$) effectively passivated perovskite films by interacting with uncoordinated $Pb^{2+}$ as its Lewis base property. Carboxyl (-COOH) passivated negatively charged undercoordinated halides via hydrogen bonding.[26] In fact, additional functional groups, such as carbonyl (C = O)[27] or the benzene[28] ring, can also present a positive effect in passivating perovskite defects for improving their stability. Herein, we introduced a new passivation molecule, N-(9-fluorenylmethoxycarbonyl)-L-alanine (Fmoc-Ala-OH), an alanine with Fmoc protecting group, which possess diverse and effective passivation groups. Finally, the inverted planar PSCs employing perovskite film passivated by Fmoc-Ala-OH achieved an efficiency of 21.14%, much higher than that of the control (16.18%).

## Experimental Section

### Construction of Solar Cells

Firstly, F-doped tin oxide (FTO, Nippon Sheet Glass) glass was cut into 19×19 $mm^2$ sections. Then the glass was cleaned using deionized water with detergent, deionized water, ethanol, isopropanol, and ethanol, respectively. The precursor solution was prepared by adding 1.454 g $Ni(NO_3)_2{\cdot}6H_2O$ and 0.15 g ethylenediamine into 5 mL ethylene glycol. Subsequently, the prepared solution was dropped onto the dry and clean FTO glass. After spin-coating at 5000 rpm for 30 s, the deposited film was first heated at 120℃ for 10 min on a hotplate, and then annealed at 400℃ for 1 h in muffle furnace. The perovskite in this work was tri-cationic halogenated structure, consisting of methylammonium ions ($MA^+$), formamidine ions ($FA^+$), and $Cs^+$. To prepare perovskite precursor solution, 0.1719 g FAI, 0.0224 g MABr, 0.0734 g $PbBr_2$, and 0.5071 g $PbI_2$ were dissolved in a mixture of DMSO and DMF. After dissolving, 84 µL of CsI was added. Then 60 µL of filtered precursor solution was dropped onto prepared NiO substrates and spun at 1000 rpm for 10 s and 4000 rpm for 30 s. In the spinning process, after the speed had reached 4000 rpm for 8 s, 200 µL of the prepared anti-solvent was dropped onto the film within 1 s. The anti-solvent was either pure ethyl acetate or Fmoc-Ala-OH (CSBio (Shanghai) Ltd.) in ethyl acetate with concentrations of 0.5 mg/mL, 1 mg/mL, 1.5 mg/mL, and 2 mg/mL. The perovskite films were then dried at 70℃ for 3 min and at 100℃ 10 min, respectively. Next, PCBM and BCP functional layers were deposited. Finally, a 50-nm thickness of silver was thermally evaporated to form the metal electrode.

### Characterization

XRD (D8 Advance, Bruker) and field-emission scanning electron microscopy (FESEM, SU8220, Hitachi) were used to observe the crystalline structure and morphology of perovskite films. UV–Vis spectroscopy (Cary 300, Varian) was applied for exploring optical performance of perovskite films. The carrier dynamics were investigated by steady-state photoluminescence (PL, FS5, Edinburgh) and transient time-resolved photoluminescence (TRPL, FLS980, Edinburgh). *J–V* curves of PSCs were collected on an electrochemical workstation (Keithley 2420 SourceMeter) under solar illumination (100 mW $cm^{-2}$, Oriel Sol3A, Newport Corp.). The dark *I–V* curves of the electron-only device were recorded from 0 to 3 V using the same electrochemical workstation.

Stable current output of PSCs was collected on another electrochemical workstation (IM6ex, Zahner). Electrochemical impedance spectroscopy (EIS, CHI660E, CH Instruments) was measured in the dark from 100 kHz to 1 Hz with an amplitude of 5 mV and quiet time of 2 s.

## Results and Discussion

SEM images of perovskite films passivated by different concentrations of Fmoc-Ala-OH are shown in Fig. 1. It can be clearly observed that the morphology of the films changed substantially after the introduction of Fmoc-Ala-OH. As shown in Fig. 1a, the pristine perovskite film presents some bright particles on the surface, which should be $PbI_2$ according to an early report.[29] Obviously, with the increase in Fmoc-Ala-OH, bright particles gradually disappear, and the film surface becomes smooth. When the concentration reaches 1.5 mg/mL, as shown in Fig. 1d, the bright particles almost completely disappear. However, cracks and pinholes appear as the concentration further increases to 2 mg/mL (Fig. 1d), which might be caused by excess Fmoc-Ala-OH. The results demonstrate that 1.5 mg/mL might be a suitable concentration for fabricating a highly efficient device. The cross-sectional image of device based on perovskite film modified by 1.5 mg/mL Fmoc-Ala-OH is presented in Fig. 1f; all functional layers are clear and in close contact with each other.

XRD was performed to evaluate the effect of Fmoc-Ala-OH on the crystallinity of perovskite film, as shown in Fig. 2a. The sharp diffraction peaks indicate that the prepared perovskite films have excellent crystallinity. The characteristic peaks at 14.2°, 28.5°, 31.8°, 40.5°, and 43.2° are related to the (110), (220), (310), (224), and (314) lattice planes of perovskite.[30] . The full width at half maximum (FWHM) values of the peak at 14.2° are 0.227, 0.204, 0.194, 0.182, and 0.193, respectively, for perovskite film treated by Fmoc-Ala-OH with concentrations of 0, 0.5, 1, 1.5, and 2 mg/mL. A lower FWHM indicates a better crystallinity, so suitable addition of Fmoc-Ala-OH is beneficial for the crystallinity of perovskite film. Additionally, the pristine perovskite film exhibits a diffraction peak at 12.7°, which is assigned to $PbI_2$ impurity. When the concentrations further increase to 1.5 mg/mL and 2 mg/mL, the diffraction peak of $PbI_2$ almost disappears, which indicates that Fmoc-Ala-OH amino acids can eliminate the uncoordinated $Pb^{2+}$ and inhibit the formation of $PbI_2$, which is helpful to reduce the defect density in perovskite film. This phenomenon is well matched with SEM images. The absorption spectra of perovskite film passivated by different concentrations of Fmoc-Ala-OH are presented in Fig. 2b. Significant improvement in light absorbance can be found for perovskite film treated by 1.5 mg/mL Fmoc-Ala-OH, which is beneficial to obtain a high current output device. The thickness of perovskite films does not change obviously, as shown in Figure S1, so the improvement of

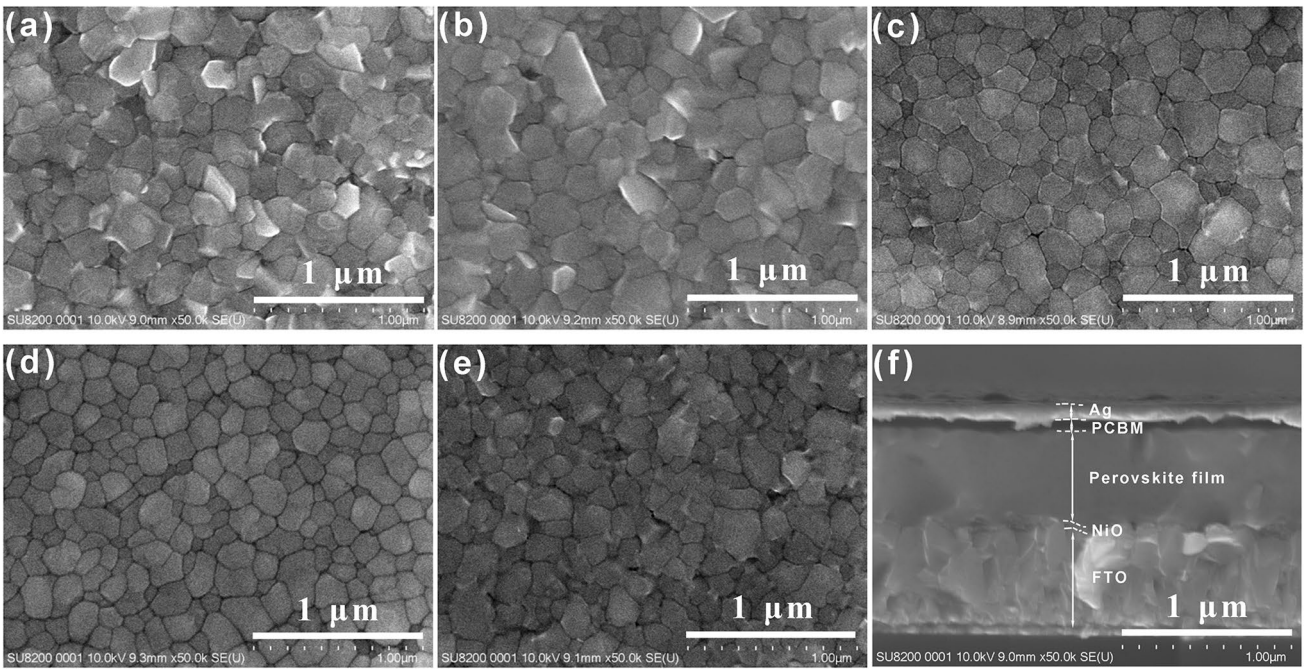


**Fig. 1** SEM images of perovskite (a) without and with Fmoc-Ala-OH passivating under different concentrations, (b) 0.5 mg /mL, (c) 1 mg/mL, (d) 1.5 mg/mL, and (e) 2 mg/mL. (f) Cross-sectional SEM images of the device based on perovskite film modified by 1.5 mg/mL Fmoc-Ala-OH.

crystallinity and components should be the main reasons for their optical performance enhancement.

The *J–V* curves of PSCs employing perovskite films with or without Fmoc-Ala-OH passivation are shown in Fig. 3a, and the corresponding photovoltaic parameters are listed in Table I. The device passivated by Fmoc-Ala-OH with 1.5 mg/mL shows the best performance, exhibiting a PCE of 21.14%, a $J_{sc}$ of 24.59 mA cm$^{-2}$, a *Voc* of 1.08, and a *FF*

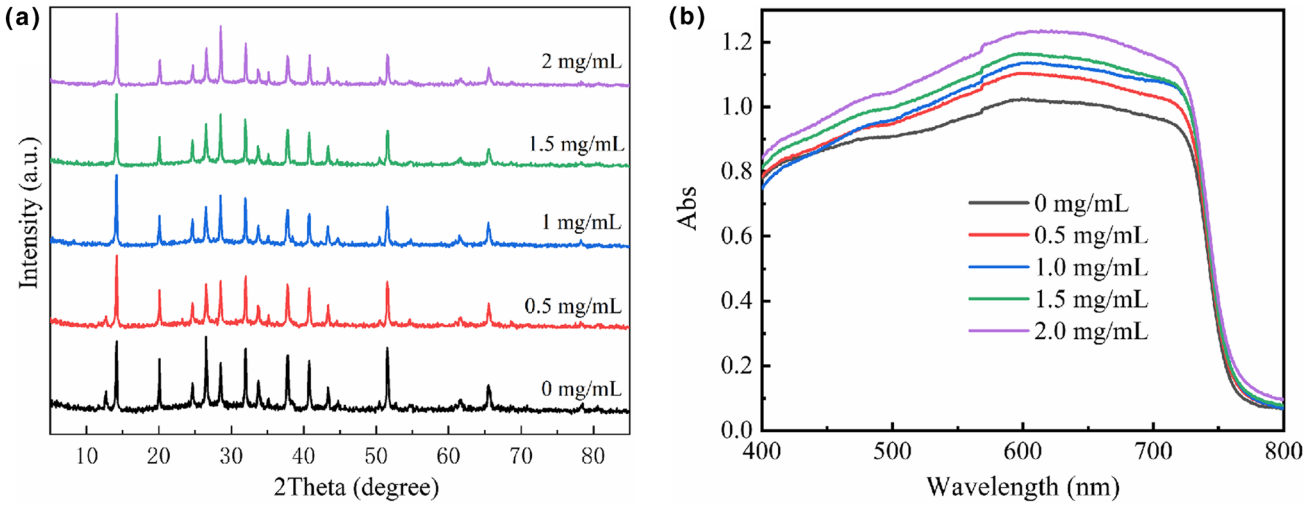


**Fig. 2** (a) XRD patterns and (b) UV–Vis spectra of perovskite films without or with treatment by different concentrations of Fmoc-Ala-OH.

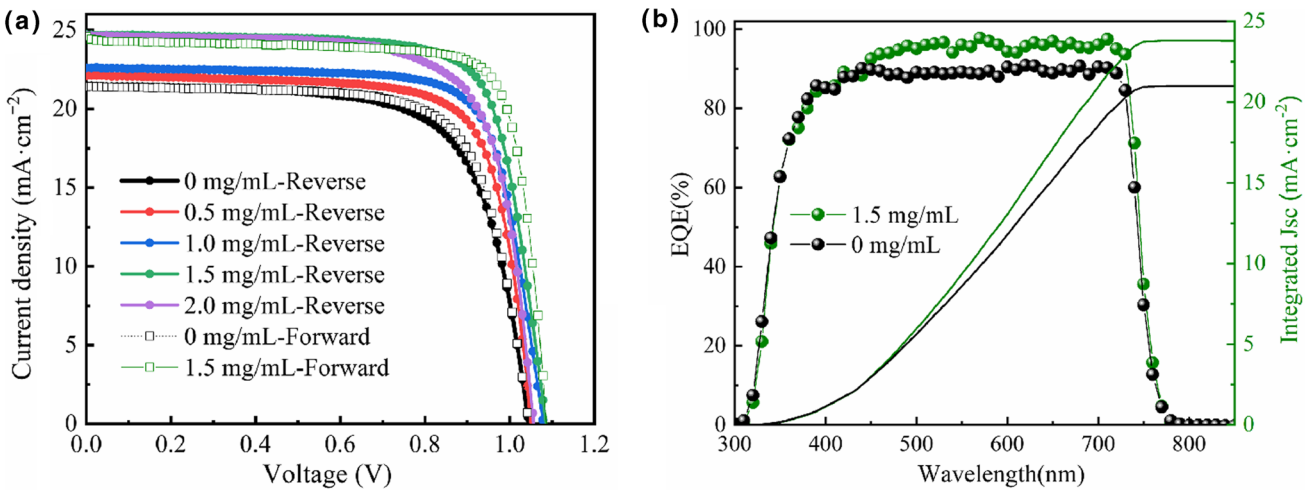


**Fig. 3** (a) *J–V* curves of perovskite solar cells based on perovskite films treated under different conditions, and IPCE curves of devices without and with modification by 1.5 mg/mL Fmoc-Ala-OH.

**Table I** Photovoltaic parameters of perovskite solar cells passivated by different concentrations of Fmoc-Ala-OH (*Voc*: open-circuit voltage, *Jsc*: short-circuit current density, *FF*: fill factor, *PCE*: photoelectric conversion efficiency).

| Concentration | Scan direction | *Voc* (V) | $J_{SC}$ (mA/cm$^2$) | *FF* (%) | *PCE* (%) |
|---|---|---|---|---|---|
| 0 mg/mL | Reverse | 1.04 | 21.46 | 69.84 | 15.63 |
| | Forward | 1.04 | 21.39 | 72.73 | 16.18 |
| 0.5 mg/mL | Reverse | 1.04 | 22.11 | 74.96 | 17.38 |
| 1.0 mg/mL | Reverse | 1.07 | 22.60 | 75.61 | 18.45 |
| 1.5 mg/mL | Reverse | 1.08 | 24.71 | 75.87 | 20.34 |
| | Forward | 1.08 | 24.59 | 79.60 | 21.14 |
| 2.0 mg/mL | Reverse | 1.05 | 24.64 | 73.08 | 19.02 |

of 79.60%. The improvement of *Jsc* might be induced by the enlarged light absorption of perovskite film after passivation process, while the enhanced *Voc* and *FF* indicate a decreased carrier recombination in the device.[31] However, as the Fmoc-Ala-OH concentration increases to 2 mg/mL, corresponding photovoltaic parameters show a downward trend. Combined with SEM image analysis, it is attributed to the cracks and deteriorated perovskite films, which can hinder the transport of carriers in the device. Moreover, we could see that the hysteresis effect of the devices under reverse and forward scan direction are low, presenting the advantage of inverted device structure. Specifically, PCE of devices based on 0 and 1.5 mg/mL are 15.63% and 20.34% under reverse scan, while the values are 16.18% and 21.14% under forward scan. IPCE spectra are presented in Fig. 3b, and we find that photon conversion efficiency is high between 400 and 700 nm for the prepared devices. The integrated *Jsc* based on the IPCE curves are 21.01 mA $cm^{-2}$ and 23.80 mA $cm^{-2}$, respectively, and the difference of these integrated values and the tested Jsc by *J*–*V* curves is within the deviation range of 5%. Ten independent devices based on perovskite films without or with modification by 1.5 mg/mL Fmoc-Ala-OH were prepared and their photovoltaic parameters were recorded, as shown in Fig. 4. The statistic results show that the modified devices do have better photovoltaic performance than the pristine one, demonstrating the advantage of introducing Fmoc-Ala-OH in device preparation.

To investigate the function of Fmoc-Ala-OH on the interface of devices and the origin of performance enhancement, we thoroughly explored the fluorescence properties of perovskite films by PL and TRPL measurement. The tested samples were prepared without a charge transport layer, so the fluorescence intensity of perovskite film was directly related to carrier radiative recombination.[25] As all samples are irradiated by the same light power, a weaker PL peak means more non-radiative carrier recombination, which can be induced by defects in the bulk or surface of perovskite film.[32,33] As shown in Fig. 5a, PL intensities increase greatly

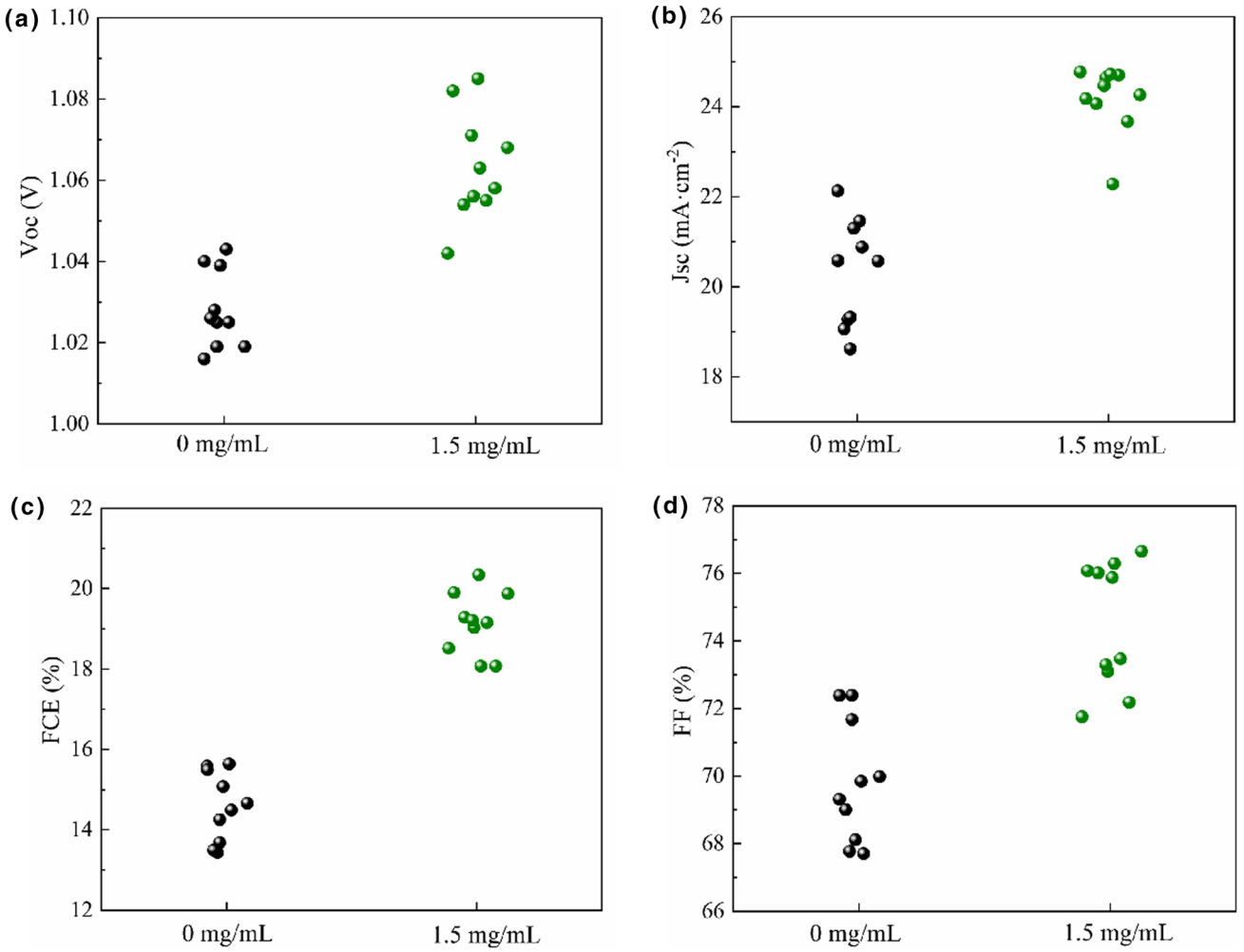


**Fig. 4** Photovoltaic parameters of 10 independent devices, (a) *Voc*, (b) *Jsc*, (c) PCE, and (d) FF.

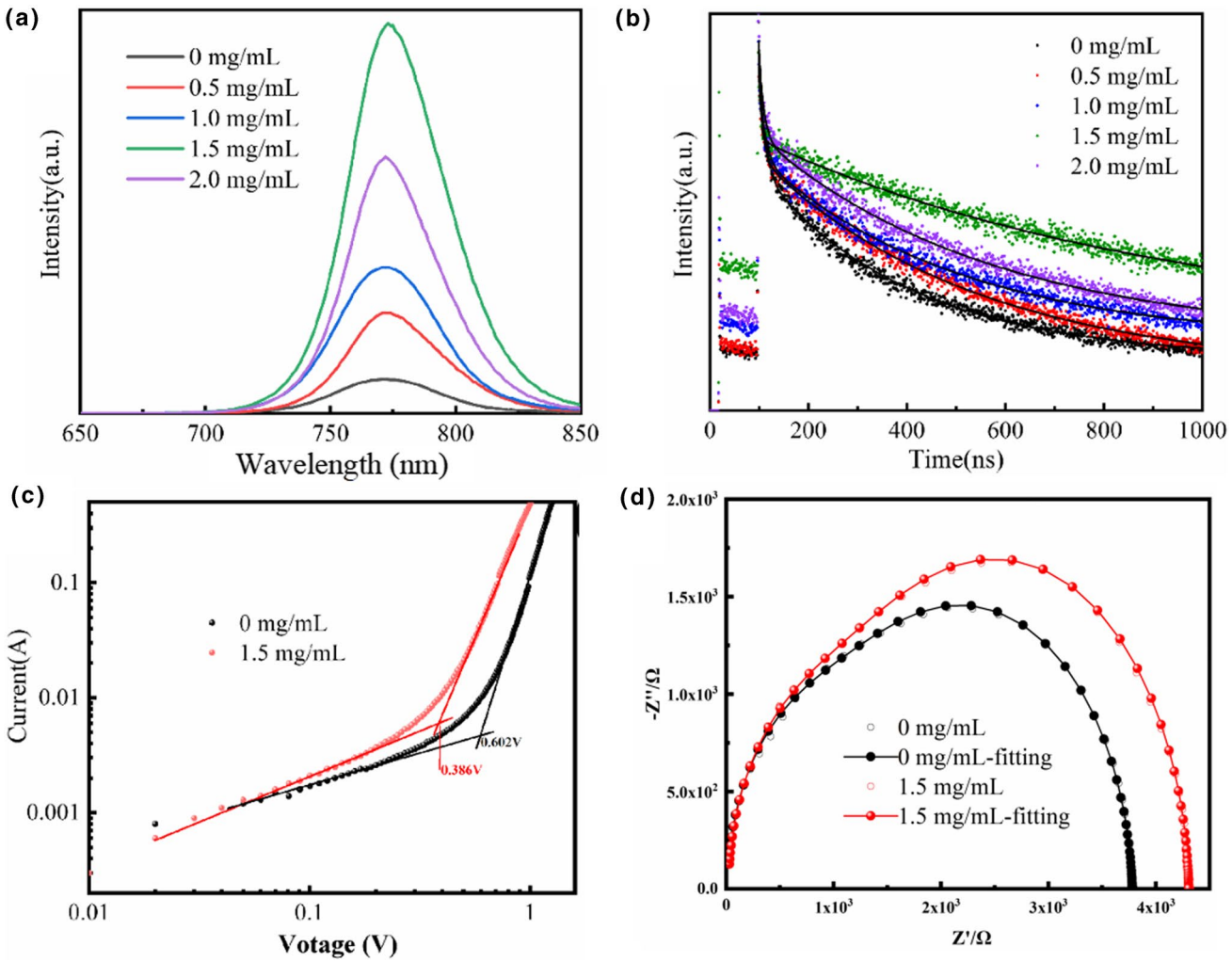


**Fig. 5** (a) Steady-state photoluminescence spectra, (b) transient time-resolved photoluminescence spectrum, (c) *I–V* curves of electron-only devices in the dark state, and (d) Nyquist plots and fitting results of different devices.

after introduction of Fmoc-Ala-OH on the surface of perovskite films, and the optimal one is achieved when the concentration is 1.5 mg/mL, which is in accordance with their corresponding device performance. It has been reported that interface passivation can reduce the trap states and retard the recombination in perovskite film, resulting in a high PL intensity.[34,35] . Time-resolved photoluminescence spectroscopy (TRPL) are shown in Fig. 4b, which present bi-exponential decay behavior. It can be fitted with the equation,

$$n(t) = A_1\exp\left(-t/\tau_1\right) + A_2\exp\left(-t/\tau_2\right) \quad (1)$$

The fast decay life parameter (τ1) represents the trap states quenching or charge transfer, while the slow decay parameter (τ2) reflects bimolecular radiative recombination.[36–38] . Carrier lifetime parameters of the perovskite films based on varied concentration of Fmoc-Ala-OH are summarized in Table II. Compared with the control, the perovskite film passivated by 1.5 mg/mL amino acid has the highest lifetime, indicating the fewest defects in the film. Based on the data shown in Table II, we believe that the passivation process does improve perovskite surface properties.

**Table II** Fitting data of TRPL spectrum.

| Concentration (mg/mL) | $\tau_1$ (ns) | $\tau_2$ (ns) | $A_1$ (%) | $A_2$ (%) | $\tau_{ave}$ (ns) |
|---|---|---|---|---|---|
| 0 | 15.86 | 329.71 | 2.93 | 97.07 | 320.47 |
| 0.5 | 13.45 | 428.03 | 1.58 | 98.42 | 421.49 |
| 1 | 10.03 | 460.00 | 0.93 | 99.07 | 455.81 |
| 1.5 | 4.95 | 856.29 | 0.27 | 99.73 | 854.01 |
| 2 | 16.92 | 509.79 | 1.17 | 98.83 | 504.02 |

In order to verify the effect of Fmoc-Ala-OH molecule on the trap state density of perovskite films, space charge

limited current (SCLC) measurement in the dark based on the electron-only device was implemented, as shown in Fig. 5c. The sample structure was FTO/PCBM/perovskite film/PCBM/Ag. The low bias section means ohmic reply, and the image shows an inflection point where the current increases rapidly, which is called the defect trap filling voltage ($V_{\mathrm{TFL}}$).[39] The value of $V_{TFL}$ is directly related to the density of defect states ($n_t$) in the device ($V_{\mathrm{TFL}} = \frac{en_tL^2}{2\varepsilon\varepsilon_0}$). The $V_{TFL}$ resulting from the intersection of tangents are marked in Fig. 5c. The $V_{\mathrm{TFL}}$ of the devices with and without Fmoc-Ala-OH passivation are 0.602 V and 0.386 V, respectively. The decreased $V_{\mathrm{TFL}}$ value indicates that the perovskite layer passivated by Fmoc-Ala-OH has lower internal defects, which could decrease the recombination of charge carriers. To further obtain insights into the charge transport process in perovskite solar cells, electrochemical impedance spectroscopy (EIS) measurement was performed and the fitting results are shown in Table III. The response impedance ($Z = Z' + iZ''$) of a device can be explored by applying high- to low-frequency conversion AC voltages to the device, which is a useful technique for analyzing charge transfer.[40–45] By observing the fitted Nyquist plots and corresponding values, the sheet resistance (Rs) of the device changes negligibly, indicating that the passivation process does not enlarge the resistance of the device. However, after modification with Fmoc-Ala-OH, charge transfer resistance (Rct) of the device decreases from 2740 Ω to 1118 Ω, and the recombination resistance (Rrec) of the device increases from 1020 Ω to 3167 Ω. According to other report,[46] a lower Rct value means a more efficient charge transfer at interfaces and a higher Rrec represents less recombination in the device. The results further prove that addition of Fmoc-Ala-OH amino acid can inhibit the recombination of charge carriers, improve the charge transfer performance of the device, and finally enhance the performance of the PSCs.

**Table III** EIS parameters of PSCs based on perovskite film without or with treatment of 1.5 mg/mL Fmoc-Ala-OH.

| Concentration | Rs (Ω) | Rct (Ω) | Rrec (Ω) |
|---|---|---|---|
| 0 mg/mL | 12.60 | 2740 | 1020 |
| 1.5 mg/mL | 20.99 | 1118 | 3167 |

It is the long duration of working stability that determines the future application of perovskite solar cells. Here, we recorded the device efficiency change within 10 days with a time interval of 24 h, as shown in Fig. 6a. We find that the control device maintained 72% of the initial efficiency after 10 days in room temperature and humidity of 38 ± 5% without encapsulation. The value increases to 80% for the device modified by 1.5 mg/mL Fmoc-Ala-OH. So, the passivation process by Fmoc-Ala-OH not only increased the device performance, but also enhanced its working stability, because the defects in perovskite film are one of the main factors for efficiency degradation. We also investigated the continuous current output of PSCs under illumination, as shown in Fig. 6b. The applied voltages on the devices are determined by the highest power output point in *J–V* curves. The results demonstrate that the device with modification by Fmoc-Ala-OH presents more stable current output compared to the control. The current is about 23.04 mA $cm^{-2}$, considering the applied voltage of 0.91 V, so the stable power output is about 20.97 mW $cm^{-2}$, which is close to the one measured by *J–V* curves.

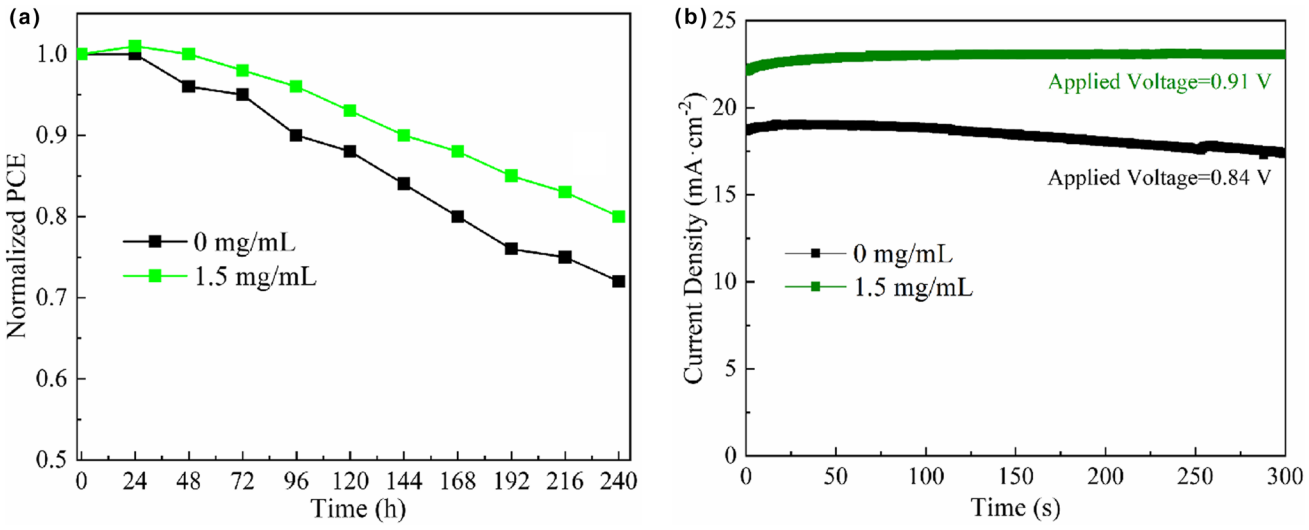


**Fig. 6** (a) Device working stability (b) current output of PSCs with or without Fmoc-Ala-OH modification under room temperature without encapsulation.

Research on functional molecules to passivate perovskite films is essential for highly efficient and stable perovskite solar cells. It has been proved that some typical functional groups have an excellent effect on specific defect types. It is meaningful to prepare molecules with integrated varieties of functional groups to adequately passivate defects in perovskite films. Meanwhile, it is also important to investigate synergistic effect of different groups in passivating defects.

## Conclusion

The inverted planar PSCs based on perovskite film passivated by Fmoc-Ala-OH in anti-solvent process is presented. It was found that 1.5 mg/mL was the optimal concentration for perovskite film modification. We find that Fmoc-Ala-OH improved the perovskite crystallizing process, reduced $PbI_2$ impurity, increased light absorption, enhanced luminescence and prolonged carrier lifetime of perovskite films. We also demonstrate that Fmoc-Ala-OH diminished defect density in perovskite film, promoted carrier transfer and decreased carrier recombination at interfaces in perovskite solar cells. Finally, the champion PSC exhibits a PCE of 21.14%, a $J_{sc}$ of 24.59 mA $cm^{-2}$, a Voc of 1.08, and a *FF* of 79.60%, all of which are higher than that of the control. Moreover, after modifying by Fmoc-Ala-OH, the device performed with enhanced working stability and a stable current output, indicating the potential of Fmoc-Ala-OH in passivating perovskite films.

**Supplementary Information** The online version contains supplementary material available at https://doi.org/10.1007/s11664-023-10265-5.

**Acknowledgments** We appreciate the Fundamental Research Funds for the Central Universities (2018QNA06).

**Conflict of interest** The authors declare that they have no conflict of interest.

## References

1. N. Imanuella, T. Witoon, Y.W. Cheng, C.C. Chong, K.H. Ng, I.M. Gunamantha, D.V.N. Vo, A.T. Hoang, and Y.K. Lai, Interfacial-engineered $CoTiO_3$-based composite for photocatalytic applications: a review. *Environ. Chem. Lett.* 20, 3039 (2022).
2. M. Jurcevic, S. Nizetic, D. Coko, M. Arici, A.T. Hoang, E. Giama, and A. Papadopoulos, Techno-economic and environmental evaluation of photovoltaic-thermal collector design with pork fat as phase change material. *Energy* 254, 124284 (2022).
3. J. Song, S. Li, Y. Zhao, J. Yuan, Y. Zhu, Y. Fang, L. Zhu, X. Gu, and Y. Qiang, Performance enhancement of perovskite solar cells by doping $TiO_2$ blocking layer with group VB elements. *J. Alloys Compd.* 694, 1232 (2017).
4. S. Huang, H. Shan, W. Xuan, W. Xu, D. Hu, L. Zhu, C. Huang, W. Sui, C. Xiao, Y. Zhao, Y. Qiang, X. Gu, J. Song, and C. Zhou C, High-performance humidity sensor based on $CsPdBr_3$ nanocrystals for noncontact sensing of hydromechanical characteristics of unsaturated soil. *Phys. Status Solidi-R* 16, 2200017 (2022).
5. H. Shan, W. Xuan, Z. Li, D. Hu, X. Gu, and S. Huang, Room temperature hydrogen sulfide sensor based on tributyltin oxide-functionalized perovskite $CsPbBr_3$ quantum dots. *ACS Appl. Nano Mater.* 5, 6801 (2022).
6. B. Cai, Y. Xing, Z. Yang, W. Zhang, and J. Qiu, High performance hybrid solar cells sensitized by organolead halide perovskites. *Energy Environ. Sci.* 6, 1480 (2013).
7. S.F. Ahmed, N. Islam, P.S. Kumar, A.T. Hoang, M. Mofijur, A. Inayat, G.M. Shafiullah, D.-V.N. Vo, I.A. Badruddin, and S. Kamangar, Perovskite solar cells: thermal and chemical stability improvement, and economic analysis. *Mater. Today Chem.* 27, 101284 (2023).
8. L. Zhao, X. Sun, Q. Yao, S. Huang, L. Zhu, J. Song, Y. Zhao, and Y. Qiang, Field-effect control in hole transport layer composed of Li:NiO/NiO for high-efficient inverted planar perovskite solar cell. *Adv. Mater. Interfaces* 9, 2101562 (2022).
9. Y. Chen, Z. Yang, S. Wang, X. Zheng, Y. Wu, N. Yuan, W. Zhang, and S. Liu, Design of an inorganic mesoporous hole-transporting layer for highly efficient and stable inverted perovskite solar cells. *Adv. Mater.* 30, 1805660 (2018).
10. Y. Qin, J. Song, Q. Qiu, Y. Liu, Y. Zhao, L. Zhu, and Y. Qiang, High-quality NiO thin film by low-temperature spray combustion method for perovskite solar cells. *J. Alloys Compd.* 810, 151970 (2019).
11. L. Zhao, J. Mou, L. Zhu, and J. Song, Synergistic effect of NiO and Spiro-OMeTAD for hole transfer in perovskite solar cell. *J. Electron. Mater.* 50, 6512 (2021).
12. J. Huang, Y. Shao, and Q. Dong, Organometal trihalide perovskite single crystals: a next wave of materials for 25% efficiency photovoltaics and applications beyond? *J. Phys. Chem. Lett.* 6, 3218 (2015).
13. I.L. Braly, D.W. deQuilettes, L.M. Pazos-Outon, S. Burke, M.E. Ziffer, D.S. Ginger, and H.W. Hillhouse, Hybrid perovskite films approaching the radiative limit with over 90% photoluminescence quantum efficiency. *Nat. Photon.* 12, 355 (2018).
14. K. Sun, J. Chang, F.H. Isikgor, P. Li, and J. Ouyang, Efficiency enhancement of planar perovskite solar cells by adding zwitterion/LiF double interlayers for electron collection. *Nanoscale* 7, 896 (2015).
15. Y. Yang, H. Peng, C. Liu, Z. Arain, Y. Ding, S. Ma, X. Liu, T. Hayat, A. Alsaedi, and S. Dai, Bi-functional additive engineering for high-performance perovskite solar cells with reduced trap density. *J. Mater. Chem. A* 7, 6450 (2019).
16. T. Du, W. Xu, M. Daboczi, J. Kim, S. Xu, C.T. Lin, H. Kang, K. Lee, M.J. Heeney, J.S. Kim, J.R. Durrant, and M.A. McLachlan, P-doping of organic hole transport layers in P-I-N perovskite solar cells: correlating open-circuit voltage and photoluminescence quenching. *J. Mater. Chem. A* 7, 18971 (2019).
17. J. Lee, H. Kang, G. Kim, H. Back, J. Kim, S. Hong, B. Park, E. Lee, and K. Lee, Achieving large-area planar perovskite solar cells by introducing an interfacial compatibilizer. *Adv. Mater.* 29, 1606363 (2017).
18. M. Tang, B. He, D. Dou, Y. Liu, J. Duan, Y. Zhao, H. Chen, and Q. Tang, Toward efficient and air-stable carbon-based all-inorganic perovskite solar cells through substituting $CsPbBr_3$ films with transition metal ions. *Chem. Eng. J* 375, 121930 (2019).
19. W. Ke, C. Xiao, C. Wang, B. Saparov, H. Duan, D. Zhao, Z. Xiao, P. Schulz, S. Harvey, W. Liao, W. Meng, Y. Yu, A. Cimaroli, C. Jiang, K. Zhu, M. Al-Jassim, G. Fang, D.B. Mitzi, and Y. Yan, Employing lead thiocyanate additive to reduce the hysteresis and boost the fill factor of planar perovskite solar cells. *Adv. Mater.* 28, 5214 (2016).

20. X. Yao, L. Zheng, X. Zhang, W. Xu, W. Hu, and X. Gong, Efficient perovskite solar cells through suppressed nonradiative charge carrier recombination by a processing additive. *ACS Appl. Mater. Interfaces* 11, 40163 (2019).
21. Y. Liu, W. Xiang, S. Mou, H. Zhang, and S. Liu, Synergetic surface defect passivation towards efficient and stable inorganic perovskite solar cells. *Chem. Eng. J.* 447, 137515 (2022).
22. Q. Chen, G. Zhai, J. Ren, Y. Huo, Z. Yun, H. Jia, Y. Gao, C. Yu, and B. Xu, Surface passivation of perovskite films by potassium bis(fluorosulfonyl) imide for efficient solar cells. *Org. Electron.* 107, 106544 (2022).
23. P. Zhang, J. Chen, L. Song, N. Gu, P. Du, X. Chen, L. Zha, W. Chen, and J. Xiong, Passivation of perovskite surfaces using 2-hydroxyacetophenone to fabricate solar cells with over 20.7% efficiency under air environment. *Appl. Surf. Sci.* 598, 153842 (2022).
24. B. Ma, X. Sun, S. Yan, L. Zhang, S. Chen, X. Liu, and J. Song, Interface modification by Fmoc-Met-OH molecule for high-efficient perovskite solar cells. *J. Mater. Sci-Mater. Electron.* 33, 15359 (2022).
25. J. Song, Q. Qiu, X. Sun, and L. Wang, Surface modification of perovskite film by an amino acid derivative for perovskite solar cell. *Org. Electron.* 108, 106598 (2022).
26. S. Yang, J. Dai, Z.H. Yu, Y. Shao, Y. Zhou, X. Xiao, X. Zeng, and J. Huang, Tailoring passivation molecular structures for extremely small open-circuit voltage loss in perovskite solar cells. *J. Am. Chem. Soc.* 141, 2781 (2019).
27. M.J. Choi, Y.S. Lee, I.H. Cho, S. Kim, D. Kim, S. Kwon, and S.I. Na, Functional additives for high-performance inverted planar perovskite solar cells with exceeding 20% efficiency: selective complexation of organic cations in precursors. *Nano Energy* 71, 104639 (2020).
28. W.Y. Zhang, L. He, D.Y. Tang, and X. Li, Surfactant sodium dodecyl benzene sulfonate improves the efficiency and stability of air-processed perovskite solar cells with negligible hysteresis. *Solar RRL* 4, 2000376 (2020).
29. X. Yang, D. Luo, Y. Xiang, L. Zhao, M. Anaya, Y. Shen, J. Wu, W. Yang, Y.-H. Chiang, Y. Tu, R. Su, Q. Hu, H. Yu, G. Shao, W. Huang, T.P. Russell, Q. Gong, S.D. Stranks, W. Zhang, and R. Zhu, Buried interfaces in halide perovskite photovoltaics. *Adv. Mater.* 33, 2006435 (2021).
30. L.C. Chen, and C.Y. Weng, Optoelectronic properties of $MAPbI_3$ perovskite/titanium dioxide heterostructures on porous silicon substrates for cyan sensor applications. *Nanoscale Res. Lett.* 10, 404 (2015).
31. J. Song, L. Zhao, S. Huang, X. Yan, Q. Qiu, Y. Zhao, L. Zhu, Y. Qiang, H. Li, and G. Li, A $p\text{-}p^+$ homojunction enhanced hole transfer in inverted planar perovskite solar cells. *Chemsuschem* 14, 1396 (2021).
32. Y. Ogomi, A. Morita, S. Tsukamoto, T. Saitho, Q. Shen, T. Toyoda, K. Yoshino, S.S. Pandey, T. Ma, and S. Hayase, All-solid perovskite solar cells with $HOCO\text{-}R\text{-}NH_3^+I^-$ anchor-group inserted between porous Titania and perovskite. *J. Phys. Chem. C* 118, 16651 (2014).
33. Q. Qiu, H. Liu, Y. Qin, C. Ren, and J. Song, Efficiency enhancement of perovskite solar cells based on $Al_2O_3$ passivated nanonickel oxide film. *J. Mater. Sci.* 55, 13881 (2020).
34. L. Zuo, Z. Gu, T. Ye, W. Fu, G. Wu, H. Li, and H. Chen, Enhanced photovoltaic performance of $CH_3NH_3PbI_3$ perovskite solar cells through interfacial engineering using self-assembling monolayer. *J. Am. Chem. Soc.* 137, 2674 (2015).
35. J. Song, Y.F. Ren, S.J. Gong, L. Zhao, W.F. Xuan, L. Zhu, Y.L. Zhao, Y.H. Qiang, L.L. Gao, and S. Huang, Performance enhancement of crystal silicon solar cell by a CsPbBr 3-Cs4PbBr6 perovskite quantum dot@ZnO/ethylene vinyl acetate copolymer downshifting composite film. *Solar RRL* 6, 2200336 (2022).
36. Q. Cui, L. Zhao, X. Sun, Q. Yao, S. Huang, L. Zhu, Y. Zhao, J. Song, and Y. Qiang, Charge transfer modification of inverted planar perovskite solar cells by $NiO_x$/Sr:$NiO_x$ bilayer hole transport layer. *Chin. Phys. B* 31, 038801 (2022).
37. S. Kanaya, G.M. Kim, M. Ikegami, T. Miyasaka, K. Suzuki, Y. Miyazawa, H. Toyota, K. Osonoe, T. Yamamoto, and K. Hirose, Proton irradiation tolerance of high-efficiency perovskite absorbers for space applications. *J. Phys. Chem. Lett.* 10, 6990 (2019).
38. X. Qi, T. Zhang, F. Tan, Y. Mei, J. Huang, G. Yue, Y. Gao, R. Liu, C. Dong, L. Zhang, and W. Zhang, Self-passivated hybrid perovskite films for improved photovoltaic performance of solar cells. *J. Mater. Sci.* 56, 6374 (2021).
39. Y. Lv, B. Cai, Q. Ma, Z. Wang, J. Liu, and W. Zhang, Highly crystalline Nb-doped $TiO_2$ nanospindles as superior electron transporting materials for high-performance planar structured perovskite solar cells. *RSC Adv.* 8, 20982 (2018).
40. H. Kim, I. Mora-Sero, V. Gonzalez-Pedro, F. Fabregat-Santiago, E.J. Juarez-Perez, N.G. Park, and J. Bisquert, Mechanism of carrier accumulation in perovskite thin-absorber solar cells. *Nat. Commun.* 4, 2242 (2013).
41. A. Dualeh, T. Moehl, N. Tétreault, J. Teuscher, P. Gao, M.K. Nazeeruddin, and M. Grätzel, Impedance spectroscopic analysis of lead iodide perovskite-sensitized solid-state solar cells. *ACS Nano* 8, 362 (2013).
42. X. Xu, H. Zhang, K. Cao, J. Cui, J. Lu, X. Zeng, Y. Shen, and M. Wang, Lead methylammonium triiodide perovskite-based solar cells: an interfacial charge-transfer investigation. *Chemsuschem* 7, 3088 (2014).
43. J. Song, Y. Yang, Y. Zhao, M. Che, L. Zhu, X. Gu, and Y. Qiang, Morphology modification of perovskite film by a simple post-treatment process in perovskite solar cell. *Mater. Sci. Eng. B* 217, 18 (2017).
44. D.H. Sin, H. Ko, S.B. Jo, M. Kim, G.Y. Bae, and K. Cho, Decoupling charge transfer and transport at polymeric hole transport layer in perovskite solar cells. *ACS Appl. Mater. Interfaces* 8, 6546 (2016).
45. Y. Xiao, G. Han, Y. Chang, H. Zhou, M. Li, and Y. Li, An all-solid-state perovskite-sensitized solar cell based on the dual function polyaniline as the sensitizer and p-type hole-transporting material. *J. Power Sources* 267, 1 (2014).
46. R.S. Sanchez, V. Gonzalez-Pedro, J.W. Lee, N.G. Park, Y.S. Kang, I. Mora-Sero, and J. Bisquert, Slow dynamic processes in lead halide perovskite solar cells characteristic times and hysteresis. *J. Phys. Chem. Lett.* 5, 2357 (2014).